Tumor necrosis and ascites on baseline ^{18}F-FDG PET/CT as independent prognostic imaging markers for double/triple-hit lymphoma

Yue Teng[1] MD,
Chong Jiang[2] MD,
Ruihe Lai[1] MD,
Zitong Zhang[2] MD,
Ming Jiang[3] MD,
Chongyang Ding[4] MD,
Zhengyang Zhou[5] MD

1. Department of Nuclear Medicine, Nanjing Drum Tower Hospital, Affiliated Hospital of Medical School, Nanjing University of Chinese Medicine, Nanjing, China
2. Department of Nuclear Medicine, West China Hospital, Sichuan University, Chengdu, China
3. Department of Medical Oncology of Cancer Center, West China Hospital, Sichuan University, Chengdu, China
4. Department of Nuclear Medicine, the First Affiliated Hospital of Nanjing Medical University, Jiangsu Province Hospital, Nanjing, China
5. Department of Radiology, Nanjing Drum Tower Hospital, Affiliated Hospital of Medical School, Nanjing University of Chinese Medicine, Nanjing, China

Keywords: ^{18}F-FDG PET/CT - Double and triple hit lymphoma - Tumor Necrosis - Ascites - Prognosis

Corresponding author:
Ming Jiang MD,
Department of Medical Oncology of Cancer Center, West China Hospital, Sichuan University, Chengdu, China.
Address: No.37, Guoxue Road, Chengdu City, Sichuan Province, China, 610000.
Tel: +86-18845130337
307048372@qq.com

Chongyang Ding MD,
Department of Nuclear Medicine, First Affiliated Hospital of Nanjing Medical University, Nanjing, Jiangsu, China.
Address: No.321, Zhongshan Road, Nanjing City, Jiangsu Province, China, 210008.
Tel: +86-15771854908
chongyangding@163.com

Zhengyang Zhou MD,
Department of Radiology, Nanjing Drum Tower Hospital, Affiliated Hospital of Medical School, Nanjing University of Chinese Medicine, Nanjing, Jiangsu, China. Address: No.321, Zhongshan Road, Nanjing City, Jiangsu Province, China, 210000.
Tel: +86-18151647759
zyzhou@nju.edu.cn

Received:
22 December 2025
Accepted revised:
29 June 2026

Abstract

Objective: Double and triple hit lymphoma (DHL/THL) is a rare genetic subtype of diffuse large B-cell lymphoma (DLBCL) characterized by extremely aggressive behavior. Tumor necrosis and ascites are also commonly associated with a poor prognosis. This study aimed to assess the potential prognostic markers on baseline fluorine-18-fluorodeoxyglucose (^{18}F-FDG) positron emission tomography/computed tomography (PET/CT) in DHL/THL patients. **Subjects and Methods:** A total of 36 DHL/THL patients, with myelocytomatosis (MYC) and B-cell lymphoma 2 (BCL2) and/or B-cell lymphoma 6 (BCL6) rearrangements from 3 independent medical centers, were retrospectively studied. These patients all underwent baseline ^{18}F-FDG PET/CT scans between November 2012 and February 2024. Presence of tumor necrosis and ascites were visually assessed at PET and CT, as necrosis^{PET} and ascites^{CT}, respectively. Survival analyses were performed using Cox regression and Kaplan-Meier methods. Progression-free survival (PFS) and overall survival (OS) were used as endpoints. Time-dependent receiver operating characteristics (ROC) curves were used to assess the predictive power of necrosis^{PET} and ascites^{CT}. **Results:** Of the 36 patients, 14 experienced recurrence, and 12 died during the follow-up period. Multivariate analysis revealed that necrosis^{PET} (hazard ratio [HR]=5.272, P=0.009; HR=5.363, P=0.026) and ascites^{CT} (HR=5.558, P=0.008; HR=7.384, P=0.020) were independently prognostic factors for PFS and OS. Time-dependent ROC analysis showed that necrosis^{PET} and ascites^{CT} had good performance in predicting PFS (accuracy: 0.671-0.758) and OS (accuracy: 0.686-0.769) occurring within 1-4 years. The risk model, incorporating necrosis^{PET} and ascites^{CT}, can effectively stratify patients for PFS (χ^2=11.804, P=0.003 and χ^2=15.754, P<0.001, respectively) and OS (χ^2=20.599, P<0.001 and χ^2=18.369, P<0.001, respectively) in subgroup analyses of patients treated with R-CHOP and intensive regimens, respectively. **Conclusions:** Necrosis^{PET} and ascites^{CT} independently predict survival in DHL/THL patients and may improve risk stratification, potentially guiding personalized therapeutic strategies.

Hell J Nucl Med 2026; 29(2): 109-120 *Epub ahead of print: 6 August 2026* *Published online: 31 August 2026*

Introduction

Myelocytomatosis (MYC), B-cell lymphoma 2 (BCL2), and B-cell lymphoma 6 (BCL6) play pivotal roles in lymphomagenesis, with MYC driving genomic instability, gene amplification, and cellular proliferation, while BCL2 and BCL6 inhibit apoptosis [1]. The 2016 revised World Health Organization (WHO) guidelines for tumors of hematopoietic and lymphoid tissues introduced a new classification for tumors characterized by rearrangements of MYC and BCL2 and/or BCL6, known as double and triple hit lymphoma (DHL/THL), affecting approximately only 7%-10% of diffuse large B-cell lymphoma (DLBCL) patients [2, 3]. Patients diagnosed with DHL/THL often exhibit aggressive clinical characteristics, including advanced stage (stage III/IV), B-symptoms, elevated lactate dehydrogenase (LDH) levels, and high-risk international prognostic index (IPI) scores [3]. Several large retrospective datasets have clearly established that the outcomes of patients with DHL/THL treated with rituximab plus cyclophosphamide, doxorubicin, vincristine, and prednisone (R-CHOP) regimen are suboptimal, with 5-year overall survival (OS) and progression-free survival (PFS) rates even as low as 27% and 18%, respectively [4, 5]. Intensified regimens, such as dose-adjusted etoposide, prednisolone, vincristine, cyclophosphamide, doxorubicin, and rituximab (DA-EPOCH-R) and R-HyperCVD, have been investigated and shown to be superior to R-CHOP for PFS but not OS [6, 7]. Therefore, the selection of treatment modalities for DHL/THL patients poses a challenge, and accurately identifying their responses to treatment is crucial for guiding new therapeutic strategies and tailoring individualized therapy.

Fluorine-18-fluorodeoxyglucose (^{18}F-FDG)positron emission tomography/computed tomography (PET/CT) has become a routine tool for prognostic assessment and management in DLBCL. Volume-based parameters from baseline PET, such as total metabolic tumor volume (TMTV) and total lesion glycolysis (TLG), reflecting the tumor burden and metabolism, have been proposed as prognostic markers in lymphoma [8]. Tumor necrosis has been identified as a significant factor contributing to renewed cancer progression and treatment resistance [9]. Recent research demonstrated ^{18}F-FDG enable the identification of tumor necrosis, present in 14%-20% of DLBCL cases and strongly associated with an adverse prognosis. [10-12]. Moreover, Malignant ascites is a common occurrence in the advanced stages of cancer. This condition is characterized by the accumulation of fluid in the abdominal cavity, which results in a significant weakening of the patient's ability to combat the disease or to undergo the prescribed treatment regimen, indicating a high mortality rate and a negative impact on the patient's overall quality of life. Computed tomography scans are commonly used as a diagnostic tool to accurately assess the volume of ascites in patients [13, 14]. However, there is limited data available regarding their prognostic value in DHL/THL patients, which needs further validation.

To the best of our knowledge, this study is the first to investigate the predictive value of ^{18}F-FDG PET/CT in DHL/THL patients. The aim of this multi-center study was to demonstrate that the tumor necrosis and ascites observed on the baseline PET/CT of DHL/THL patients can serve as potential prognostic markers, aiding in risk stratification and clinical decision-making.

Subjects and Methods

Patients

A total of 36 patients diagnosed with DHL/THL from November 2012 to February 2024 were included in this retrospective study. Data were gathered from 3 independent medical centers: Nanjing University Medical School Affiliated Drum Tower Hospital (8 cases), West China Hospital of Sichuan University (12 cases), and Jiangsu Province Hospital, the First Affiliated Hospital of Nanjing Medical University (16 cases). The inclusion criteria were as follows: (I) DHL/THL was confirmed by MYC and BCL2 and/or BCL6 rearrangements via fluorescence in situ hybridization (FISH) testing; (II) baseline ^{18}F-FDG PET/CT scan was performed. Patients who had a previous malignancy, chemotherapy, radiotherapy, pregnancy or lactation, or diabetes mellitus with a fasting blood glucose level greater than 150mg/dL were excluded from this study. Clinical parameters [sex, age, LDH level, Ann Arbor stage, B symptoms, Eastern Cooperative Oncology Group Performance Status (ECOG PS), IPI score, pathological type, MYC and BCL2 protein expression, treatment] were determined from the medical records. This study was approved by the institutional review boards of each hospital involved, which waived the need for written informed consent.

^{18}F-FDG PET/CT scanning protocol

All patients fasted for at least 6 hours before scans, resulting in blood glucose levels under 8.7mmol/L. Then, 185-370MBq of ^{18}F-FDG (5.18MBq/kg) was administered intravenously. Fluorine-18-FDG PET/CT scans (from the base of the skull to the upper thigh) were performed 60 minutes after the radiopharmaceutical injection. Emission data were acquired for 2 minutes in each bed position. All patients underwent PET/CT scans with one of the following systems: Gemini GXL (Reconstruction method: ordered subset expectation maximization [OSEM], PET slice thickness: 4mm and PET pixel spacing: 4mm), UM780PET/CT (Reconstruction method: OSEM, PET slice thickness: 2.76mm and PET pixel spacing: 2.9mm), GE Discovery PET/CT Clarity 710 (Reconstruction method: VUE point FX, PET slice thickness: 3.75mm and PET pixel spacing: 5.47mm), Biograph 16 PET/CT (Reconstruction method: OSEM, PET slice thickness: 5mm and PET pixel spacing: 4mm). Computed tomography acquisition data were used for attenuation correction.

Imaging analysis

Positron emission tomography/CT images were interpreted independently by two nuclear medicine specialists who were blinded to all patient information and clinical conditions. The results were determined by a consensus reached by the 2 physicians. Necrosis PET was defined as an area of hypometabolism within the hypermetabolic tumor (Figure 1) [15]. Images were reviewed using the LIFEx-7.3.0 software (https://www.lifex-soft.org/) to calculate maximum standardized uptake value (SUVmax), metabolic tumor volume (MTV), and TLG [16]. Regions of interest (ROI) were placed manually to cover the lesion, and the SUVmax was recorded for every lesion. For each PET dataset, the SUVmax was defined as the highest SUV among all hypermetabolic tumor foci. The MTV was determined by drawing a circular volume of interest (VOI) fully encasing all involved lesions in axial, coronal, and sagittal PET/CT images. Then, the boundaries of voxels with 41% SUV were produced automatically. The TMTV was obtained by adding the MTV of all lesions. The TLG is the sum of the MTV multiplied by the SUVmean (mean of lesions) for all lesions in each patient.

Treatment

The chemotherapy regimens administered in this study comprised the standard R-CHOP regimen (n=20) and intensive regimens, which included DA-EPOCH-R (n=14) and rituximab plus hyperfractionated cyclophosphamide, vincristine, doxorubicin, and dexamethasone alternating with high-dose methotrexate and cytarabine (R-HyperCVD) (n=2).

Statistical methods

The relationships between the two groups of necrosis^{PET} and ascites^{CT} were analyzed using Fisher's exact tests and t-tests. Time-dependent receiver operating characteristics (ROC) curves were used to evaluate the predictive ability for PFS and OS in different periods. Area under the curve (AUC) was calculated accordingly. Estimates of PFS and OS were calculated via the Kaplan-Meier method, and the comparison of differences between the PFS and OS of the two groups was evaluated by the log-rank test. A univariate analysis was conducted on the PFS and OS of all clinical, pathological and

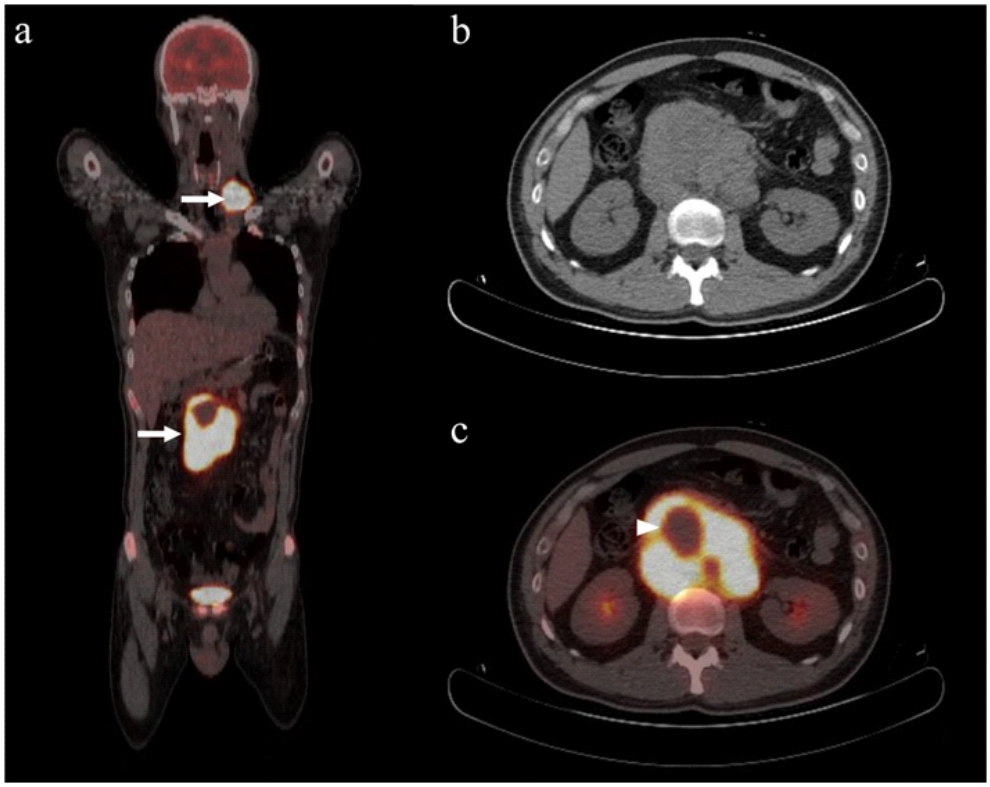

Figure 1. Assessment of tumor necrosis on ^{18}F-FDG PET/CT imaging. A 45-year-old male patient with DHL presented with tumor masses localized in the retroperitoneum and left neck. The coronal ^{18}F-FDG PET image (a) depicts the extent of the tumors (white arrows). The axial CT (b) and fused ^{18}F-FDG PET/CT (c) images further elucidate the presence of hypometabolism areas within the tumor masses located in the retroperitoneum (white arrowhead), indicative of necrotic tissue.

PET/CT parameters. Multiple Cox regression models were used to further determine the prognostic risk factors of DHL/THL. Data analysis was performed using IBM SPSS 25 and R software (version 4.2.2, www.R-project.org). A P-value less than 0.05 were considered statistically significant for all analyses.

Results

Patients' characteristics

Characteristics of 36 DHL/THL patients are summarized in Table 1, with 32 patients classified as DHL (comprising 16 patients with MYC and BCL2 rearrangements and 16 patients with MYC and BCL6 rearrangements) and 4 patients classified as THL. After a median follow-up of 27.6 months (range: 2.2-87.8 months), 14 patients had disease relapse or progression, and 12 patients died (Figure 2).

Clinical characteristics and PET parameters in relation to necrosis^{PET} and ascites^{CT}

The differences in clinical characteristics and PET parameters between the dichotomized necrosis^{PET} and ascites^{CT} groups are shown in Supplementary Table 1. The LDH level was significantly associated with necrosis^{PET} (P=0.025). Additionally, B symptoms and ECOG PS were significantly associated with ascites^{CT} (P=0.010 and P=0.003, respectively).

Univariate and multivariate analysis results

The optimal cut-off values in group of PFS, as determined by ROC curves, for SUVmax, TMTV, and TLG were found to be 12.8, 1006.9cm^3, and 6252.6, respectively. As for the group of OS, the cut-off values were 14.5, 1032.7cm3, and 7487.1, respectively. The results of the univariate analysis indicated that ECOG PS, necrosis^{PET} and ascites^{CT} were significantly correlated with both inferior PFS and OS. The univariate analysis results are presented in Table 2. Following multivariate analysis, necrosis^{PET} and ascites^{CT} remained statistically independent predictors of PFS (P=0.009 and P=0.008, respectively) and OS (P=0.026 and P=0.020, respectively), as shown in Table 3.

Survival analysis

The survival analysis revealed that patients with necrosis^{PET} or ascites^{CT} had significantly shorter PFS (P=0.001 and P< 0.001, respectively) and OS (P=0.002 and P<0.001, respectively) (Figure 3).

Time-dependent ROC analysis and risk model construction

The trends of the AUC of necrosis^{PET} and ascites^{CT} were illustrated in Figure 4. Overall, necrosis^{PET} and ascites^{CT} maintained AUC in predicting both PFS and OS over 1-4 years (PFS: 1-year [necrosis^{PET}] 0.750 > 0.677 [ascites^{CT}]; 2-year [necrosis^{PET}] 0.750 > 0.671 [ascites^{CT}]; 3-year: [ascites^{CT}] 0.736 > 0.702 [necrosis^{PET}]; 4-year [necrosis^{PET}] 0.758 > 0.690 [ascites^{CT}]);

Table 1. *Demographics and clinical characteristics of the study population.*

Characteristic		Overall patients (n=36)
Sex		
	Female/Male	18/18
Age		
	<60 years/≥60 years	23/13
LDH		
	Normal/Higher than normal	13/23
B symptoms		
	No/Yes	24/12
ECOG PS		
	0-1/≥2	26/10
Extralnode involvement		
	0-1/≥2	18/18
Ann Abor stage		
	I-II/III-IV	6/30
IPI		
	0-2/3-5	16/20
Bulky disease		
	No/Yes	27/9
Pathological type		
	GCB/non-GCB	29/7
MYC and BCL2 protein double expression		
	No/Yes	17/19
MYC、BCL2 and/or BCL6rearrangements		
	DHL/THL	32/4
Treatment		
	R-CHOP regimen/Intensive regimens	22/14

LDH, lactate dehydrogenase; ECOG PS, Eastern Cooperative Oncology Group performance status; IPI, International Prognostic Index; NCCN-IPI, National Comprehensive Cancer Network International Prognostic Index; GCB, germinal center B-cell; DHL Double Hit Lymphoma(MYC and BCL2/BCL6 rearrangements);THL Triple Hit Lymphoma(MYC and BCL2 and BCL6 rearrangements).

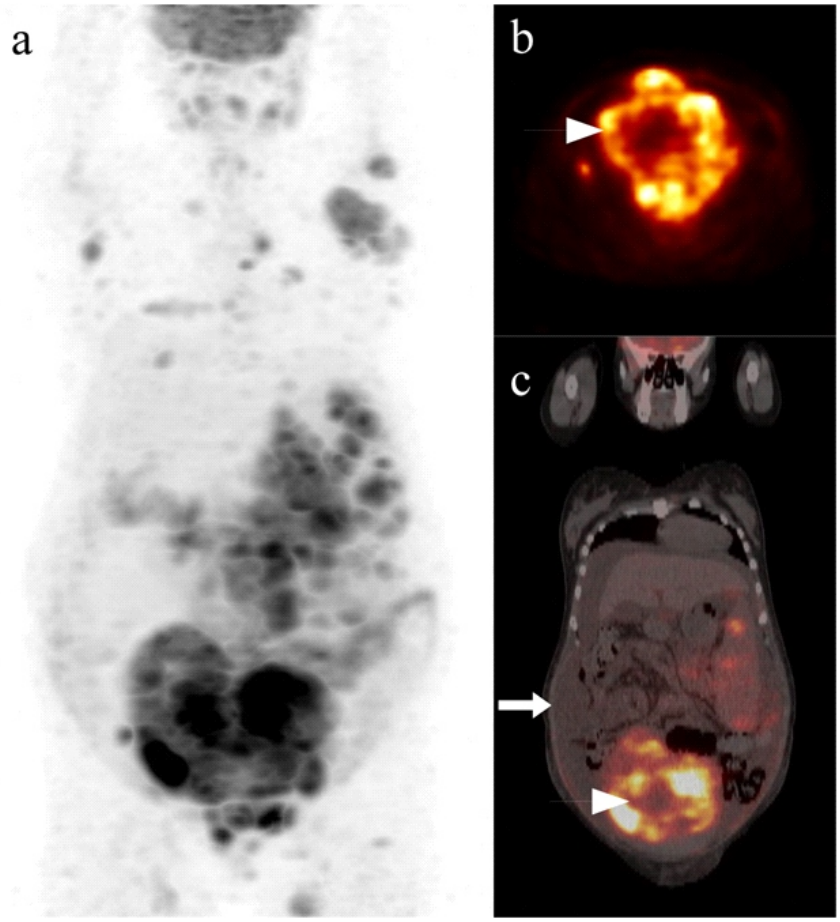

Figure 2. A 35-year-old woman with DHL presented with multiple lesions involving a large abdominal mass accompanied by significant ascites, as demonstrated on the coronal maximum intensity projection (MIP) ^{18}F-FDG PET image (a). The coronal ^{18}F-FDG PET image (b) reveals a region of hypometabolism within the hypermetabolic mass, indicative of necrotic tissue (arrows). The fused coronal ^{18}F-FDG PET/CT (c) images further clarify the presence of necrotic areas within the abdominal tumor masses (white arrowheads) and ascites (white arrows). The patient subsequently received 6 cycles of dose-adjusted etoposide, prednisolone, vincristine, cyclophosphamide, doxorubicin, and rituximab (DA-EPOCH-R) chemotherapy and experienced recurrence at 11 months, followed by death at 18 months.

OS: 1-year: [necrosis^{PET}] 0.737 > 0.686 [ascites^{CT}]; 2-year: [necrosis^{PET}] 0.769 > 0.715 [ascites^{CT}]; 3-year: [ascites^{CT}] 0.758 > 0.738 [necrosis^{PET}]; 4-year: [ascites^{CT}] 0.759 > 0.740 [necrosis^{PET}])). The accuracy, sensitivity (Se), specificity (Sp), positive predictive value (PPV), and negative predictive value (NPV) of necrosis^{PET} and ascites^{CT} for PFS and OS at 4-time points over 1-4 years are shown in Table 4.

Combining necrosis^{PET} and ascites^{CT} allowed for predictive value in stratifying patients into three risk groups: low-risk (absence of both necrosis^{PET} and ascites^{CT}, n=22), intermediate-risk (presence of either necrosis^{PET} or ascites^{CT}, n=10), and high-risk (presence of both necrosis^{PET} and ascites^{CT}, n=4). The risk model maintained a greater AUC than that of IPI in predicting both PFS and OS over 1-4 years (Figure 5).

Prognostic subanalysis between R-CHOP and intensive regimens

In the subanalysis of treatment regimens, the risk model effectively stratified DHL/THL patients in both the R-CHOP regimen and intensive regimens groups for predicting PFS (χ^2=11.804, P=0.003 and χ^2=20.599, P<0.001, respectively) and OS (χ^2=15.754, P<0.001 and χ^2=18.369, P<0.001, respectively) (Figure 6 and Table 5).

Discussion

Tumor necrosis is a common pathological phenomenon in tumors, which may be caused by metabolic stress, hypoxia, glucose deprivation, and reactive oxygen species (ROS)-mediated events in tumor tissues [17]. Research has confirmed that tumor necrosis can potentially induce a more aggressive growth pattern by stimulating cancer growth through inflammation, while also reducing responsiveness to chemotherapy and conferring inherent resistance to anti-cancer therapies [9]. Previous studies have shown that tumor necrosis is a poor prognostic risk factor for a variety of tumors, such as squamous cell carcinoma [18], nasopharyngeal carcinoma [19], sarcomas [15], non-small cell lung cancer (NSCLC) [20], glioblastoma [21]. Adams et al. used contrast-enhanced CT to observe the involved lesions in DLBCL patients and found that the presence of tumor necrosis was

Supplementary Table 1. *Comparison of patient clinical data with necrosisPETand ascitesCT.*

Patient data	Necrosis^{PET}			Ascites^{CT}		
	Absence (n=24)	Presence (n=12)	P value*	Absence (n=30)	Presence (n = 6)	P value*
Sex, F/M	15/9	3/9	0.075	15/15	3/3	1.000
Age,<60/≥60	16/8	7/5	0.720	19/11	4/2	1.000
LDH level, normal/elevated	12/12	1/11	0.025	13/17	0/6	0.068
B symptoms, No/Yes	17/7	7/5	0.497	23/7	1/5	0.010
ECOG PS, 0-1/≥2	19/5	7/5	0.247	25/5	1/5	0.003
Extralnode involvement, 0-1/≥2	13/11	5/7	0.725	16/14	2/4	0.658
Ann Abor stage, I-II/III-IV	5/19	1/11	0.640	6/24	0/6	0.561
IPI, 0-2/3-5	13/11	3/9	0.157	15/15	1/5	0.196
Bulky disease, No/Yes	20/4	7/5	0.126	24/6	3/3	0.151
Pathological type, non-GCB/GCB	6/18	1/11	0.384	7/23	0/6	0.317
MYC and BCL2 protein double expression, No/Yes	13/11	4/8	0.302	15/15	2/4	0.662
Treatment,R-CHOP regimen/Intensive regimens	13/11	9/3	0.292	19/11	3/3	0.658
SUVmax	26.26±22.26	15.93±9.22	0.079	25.24±20.20	10.68±7.51	0.175
TMTV	845.87± 1001.87	1368.13± 932.08	0.796	842.36± 865.21	1997.92± 1116.21	0.237
TLG	6755.54± 7082.44	8775.00± 5405.45	0.239	6640.84± 6258.99	9923.37± 7210.21	0.117

*LDH, lactate dehydrogenase; ECOG PS, Eastern Cooperative Oncology Group performance status; IPI, International Prognostic Index; GCB, germinal center B-cell. *P < 0.05.*

Table 2. *Univariate analysis of factors predictive of PFS and OS.*

Parameters	Progression-free survival			Overall survival		
	95% CI	HR	P value*	95% CI	HR	P value*
Sex, F/M	0.637-5.378	1.851	0.258	0.482-5.260	1.592	0.446
Age, <60/≥60	0.578-4.961	1.693	0.337	0.587-6.526	1.958	0.274
LDH level, normal/elevated	0.453-4.367	1.406	0.555	0.574-9.115	2.287	0.241
B symptoms, no/yes	0.547-4.580	1.583	0.397	0.503-5.450	1.656	0.407
ECOG PS, 0-1/≥2	1.039-10.116	3.242	0.043	1.396-17.792	4.983	0.013
Extralnode involvement, 0-1/≥2	0.527-4.744	1.581	0.414	0.612-7.665	2.166	0.231
Ann Abor stage, I-II/III-IV	0.440-26.057	3.386	0.241	0.293-18.060	2.300	0.428
IPI, 0-2/3-5	0.617-6.125	1.943	0.257	0.760-11.875	3.004	0.117
Bulky disease, no/yes	0.267-2.930	0.884	0.840	0.396-4.943	1.400	0.601
Pathological type, non-GCB/GCB	0.244-3.150	0.876	0.839	0.168-2.398	0.635	0.503
MYC and BCL2 protein double expression, no/yes	0.963-10.062	3.113	0.058	0.566-6.658	1.941	0.291
Treatment,R-CHOP regimen/Intensive regimens	0.197-1.798	0.595	0.358	0.111-1.615	0.424	0.209
NecrosisPET, absence/presence	1.799-20.287	6.041	0.004	1.723-26.529	6.761	0.006
AscitesCT, absence/presence	2.007-22.163	6.669	0.002	2.536-36.021	9.557	0.001
SUVmax	0.420-3.778	1.259	0.681	0.361-4.325	1.250	0.724
TMTV	0.400-3.342	1.156	0.789	0.556-5.978	1.823	0.322
TLG	0.346-2.954	1.011	0.983	0.561-8.065	2.127	0.267

*CI, confidence interval; SE, standard error; LDH, lactate dehydrogenase; ECOG PS, Eastern Cooperative Oncology Group performance status; IPI, International Prognostic Index; GCB, germinal center B-cell; SUVmax, maximum standardized uptake value; TMTV, total metabolic tumor volume; TLG, total lesion glycolysis.*P < 0.05.*

Table 3. *Multivariate analysis of factors predictive of survival.*

Parameters	Progression-free survival			Overall survival		
	P value*	HR	95% CI	P value*	HR	95% CI
Ascites^{CT}	0.008	5.558	1.558-19.828	0.020	7.384	1.854-29.418
Necrosis^{PET}	0.009	5.272	1.515-18.352	0.026	5.363	1.304-22.056

*CI, confidence interval; HR, hazard ratio. *P < 0.05.*

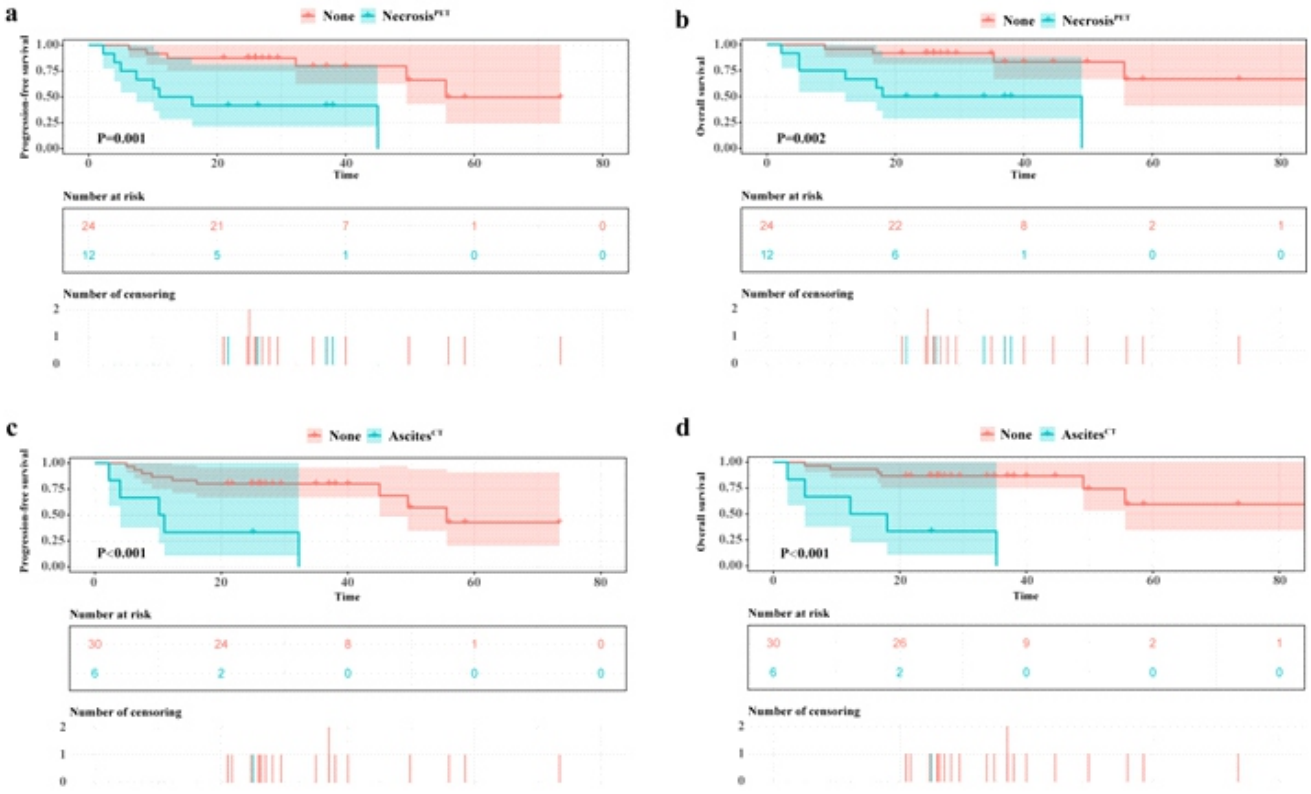

Figure 3. Kaplan-Meier plots for PFS and OS in all patients in relation to necrosis^{PET} (a, b) and ascites^{CT} (c, d).

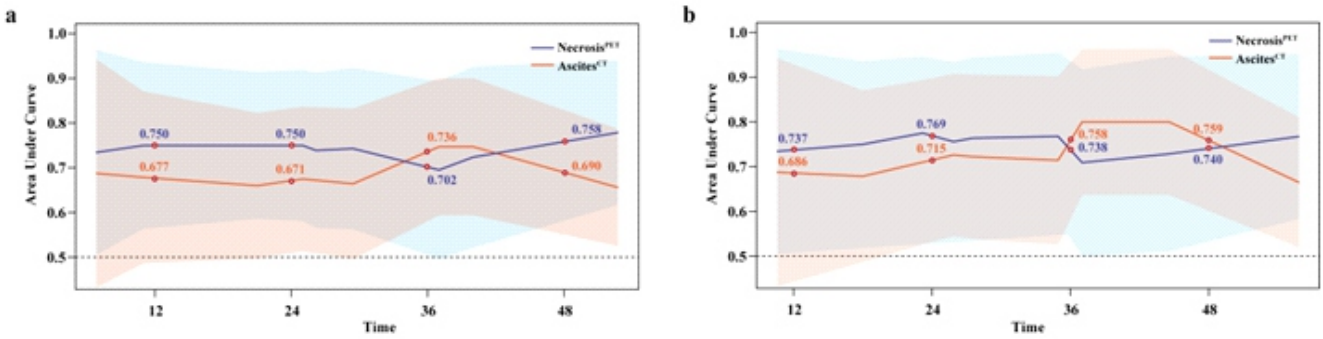

Figure 4. The AUC fluctuations of the necrosis^{PET} and ascites^{CT} for predicting PFS (a) and OS (b).

Table 4. *Prediction of outcomes with necrosis^{PET} and ascites^{CT}*

Time	PFS					OS				
	Necrosis^{PET}									
	Acc(%)	Se(%)	Sp(%)	PPV(%)	NPV(%)	Acc(%)	Se(%)	Sp(%)	PPV(%)	NPV(%)
1-year	75.0	75.0	N/A	100.0	0.0	75.0	75.0	N/A	100.0	0.0
2-year	69.2	70.0	66.7	87.5	40.0	72.7	75.0	66.7	85.7	50.0
3-year	75.0	63.6	84.6	77.8	73.3	73.9	66.7	78.6	66.7	78.6
4-year	73.3	66.7	77.8	66.7	77.8	72.4	66.7	75.0	54.5	83.3
	Ascites^{CT}									
	Acc(%)	Se(%)	Sp(%)	PPV(%)	NPV(%)	Acc(%)	Se(%)	Sp(%)	PPV(%)	NPV(%)
1-year	50.0	50.0	N/A	100.0	0.0	50.0	50.0	N/A	100.0	0.0
2-year	53.8	40.0	100.0	100.0	33.3	63.6	50.0	100.0	100.0	42.9
3-year	70.8	45.5	92.3	83.3	66.7	78.3	55.6	92.9	83.3	76.5
4-year	73.3	41.7	94.4	83.3	70.8	82.8	55.6	95.0	83.3	82.6

PFS, progression-free survival; OS, overall survival; Acc, accuracy; Se, sensitivity; Sp, specificity; PPV, positive predictive value; NPV, negative predictive value. N/A: Not available.

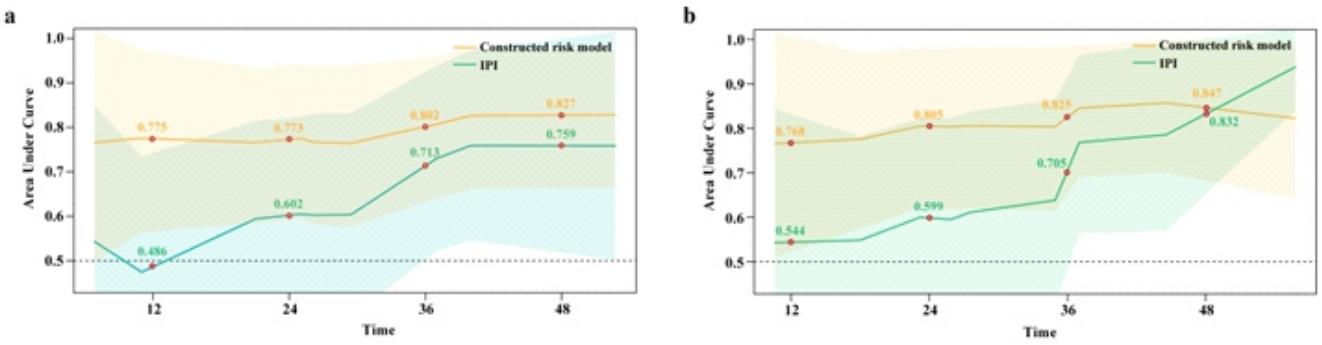

Figure 5. The AUC fluctuations of the constructed risk model and IPI for predicting PFS (a) and OS (b).

the only independent risk factor for their survival prognosis [22]. However, due to the lagging morphological changes compared to functional changes in tumors, there may be false negatives in identifying lesion necrosis. Fluorine-18-FDG PET, serving as molecular functional imaging, has been shown by several studies to accurately detect tumor necrosis with high sensitivity and specificity (88%, 81%) [23].

In the present study, we addressed the issue of prognostic stratification capacity of necrosis^{PET} on baseline ^{18}F-FDG PET/CT in patients with DHL/THL. The results indicated that patients with the presence of necrosis^{PET} had lower survival rates and that necrosis^{PET} was an independent predictor of survival outcomes after multivariate analysis. These results are consistent with previous studies supporting necrosis^{PET} as a reliable indicator for prognosis evaluation in nodal DLBCL patients [11, 12].

Malignant ascites often occurs as a symptom of the terminal stage of cancer and reduces the patient's ability to resist diseases, which is associated with a poor prognosis [13, 14]. Our study demonstrated that ascites on CT is another independent predictor of survival outcomes in DHL/THL patients, highlighting the importance of early detection and management to improve patient prognosis. Further studies are needed to determine whether the findings of our study on the prognostic value of ascites in DHL/THL patients can be extended to other non-specific DLBCL, as no relevant research literature has been found.

Total MTV and TLG derived from ^{18}F-FDG PET are powerful indices for assessing tumor burden and risk stratification in DLBCL patients. However, in the current study, we found that TMTV and TLG were not independent survival predictors of DHL/THL patients. The exact reason remains unexplained, but we observed an interesting phenomenon: the majority of included patients were at advanced stages (III-IV: 83.3%), and their TMTV (median: 732.5, range: 18.1-3566.0) and TLG (median: 6845.6, range: 58.8-23375.4) values were

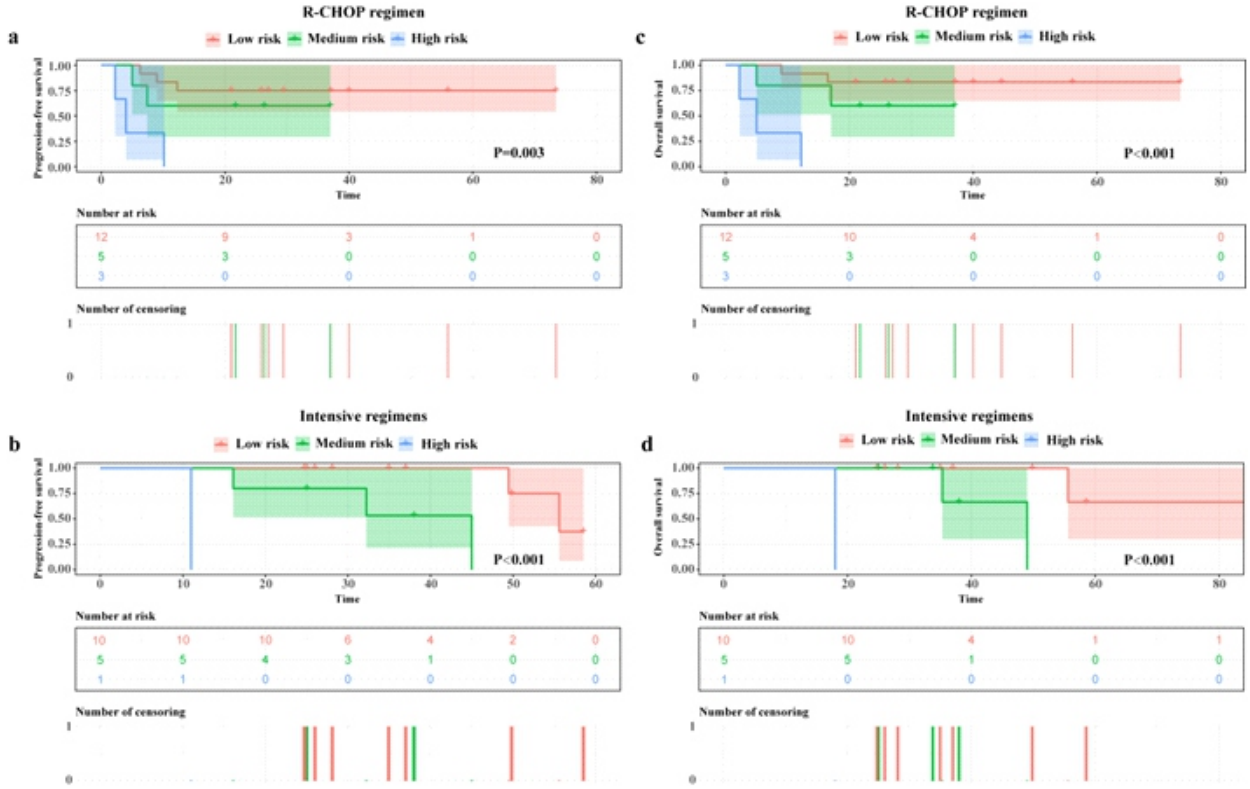

Figure 6. Kaplan-Meier survival analysis of PFS (a, b) and OS (c, d) in patients subdivided by rituximab plus cyclophosphamide, doxorubicin, vincristine, and prednisone (R-CHOP) regimen/intensive regimens group according to the constructed risk model.

Table 5. *Risk stratification of DHL/THL patients receiving R-CHOP or intensive regimens according to the combination of Necrosis^{PET} and Ascites^{CT}.*

Treatment	Group	No. of patients (n=36)	Progression-free survival			Overall survival		
			Number of events	Survival (%)	χ^2 (P value*)	Number of events	Survival (%)	χ^2 (P value*)
R-CHOP regimen	Low-risk	12	3	75.0	11.804 (0.003)	2	83.0	15.754 (<0.001)
	Medium-risk	5	2	60.0		2	60.0	
	High-risk	3	3	0.0		3	0.0	
Intensive regimens	Low-risk	10	2	80.0	20.599 (<0.001)	2	80.0	18.369 (<0.001)
	Medium-risk	5	3	40.0		2	60.0	
	High-risk	1	1	0.0		1	0.0	

**P < 0.05.*

obviously higher than those seen in other studies of DLBCL [24, 25]. This may have to some extent reduced the predictive discriminative ability of quantitative PET indices. Furthermore, despite its widespread utilization in clinical practice, the IPI did not demonstrate independent predictive value for survival in this study. Studies have indicated that the IPI inadequately identifies DLBCL patients with an unfavorable prognosis [26, 27]. This finding suggests that the unique characteristics of DHL/THL may render quantitative PET indices and IPI unsuitable as independent survival predictors.

Establishing the optimal regimens for DHL/THL presents challenges, necessitating an urgently warranted individualized approach. To enhance risk stratification efficiency, we evaluated the combined use of necrosis^{PET} and ascites^{CT} as a risk model in DHL/THL patients. Our results indicated that the risk model exhibited significant prognostic superiority over IPI in terms of time-dependent AUC. Particularly, in the treatment regimen subanalysis, the risk model effectively stratified patients, identifying those who might benefit from R-CHOP or intensive regimens, thus improving their long-term survival prospects.

Our study has several limitations, notably the relatively small number of patients analyzed, which is attributed to the rarity of the disease. Additionally, due to the retrospective nature of the study, histopathological confirmation of necrotic tumor sites was unavailable. Furthermore, variations in SUVmax measurements may arise across different PET systems due to the multi-center design of the study [28]. However, the 41% SUVmax threshold method chosen in our study has been recommended by the European Association of Nuclear Medicine for its superior interobserver agreement [29].

In conclusion, necrosis^{PET} and ascites^{CT} are independent prognostic factors of survival in DHL/THL patients. Moreover, the established risk model can stratify patients effectively, especially for patients receiving heterogeneous treatment regimens, which suggests its potential integration into decision-making to achieve a more personalized medicine approach.

The authors declare that they have no conflicts of interest.

Funding Source

This work was supported by funding for Clinical Trials Fund Project from Nanjing Drum Tower Hospital, Affiliated of Nanjing University under Grant No.2025-LCYJ-PY-19.

Bibliography

1. Riedell PA, Smith SM. Double hit and double expressors in lymphoma: Definition and treatment. *Cancer* 2018; 124(24): 4622-32.
2. Swerdlow SH, Campo E, Pileri SA et al. The 2016 revision of the World Health Organization classification of lymphoid neoplasms. *Blood* 2016; 127(20): 2375-90.
3. Landsburg DJ, Petrich AM, Abramson JS et al. Impact of oncogene rearrangement patterns on outcomes in patients with double-hit non-Hodgkin lymphoma. *Cancer* 2016; 122(4): 559-64.
4. Johnson NA, Slack GW, Savage KJ et al. Concurrent expression of MYC and BCL2 in diffuse large B-cell lymphoma treated with rituximab plus cyclophosphamide, doxorubicin, vincristine, and prednisone. *J Clin Oncol* 2012; 30(28): 3452-9.
5. Oki Y, Noorani M, Lin P et al. Double hit lymphoma: the MD Anderson Cancer Center clinical experience. *Br J Haematol* 2014; 166(6): 891-901.
6. Petrich AM, Gandhi M, Jovanovic B et al. Impact of induction regimen and stem cell transplantation on outcomes in double-hit lymphoma: a multicenter retrospective analysis. *Blood* 2014; 124(15): 2354-61.
7. Howlett C, Snedecor SJ, Landsburg DJ et al. Front-line, dose-escalated immunochemotherapy is associated with a significant progression-free survival advantage in patients with double-hit lymphomas: a systematic review and meta-analysis. *Br J Haematol* 2015; 170(4): 504-14.
8. Kostakoglu L, Chauvie S. PET-Derived Quantitative Metrics for Response and Prognosis in Lymphoma. *PET Clin* 2019; 14(3): 317-29.
9. Karsch-Bluman A, Benny O. Necrosis in the Tumor Microenvironment and Its Role in Cancer Recurrence. *Adv Exp Med Biol* 2020; 1225: 89-98.
10. Song MK, Chung JS, Shin DY et al. Tumor necrosis could reflect advanced disease status in patients with diffuse large B cell lymphoma treated with R-CHOP therapy. *Ann Hematol* 2017; 96(1): 17-23.
11. Adams HJA, de Klerk JMH, Fijnheer R et al. Tumor necrosis at ^{18}F-FDG-PET is an independent predictor of outcome in diffuse large B-cell lymphoma. *Eur J Radiol* 2016; 85(1): 304-9.
12. Kahle XU, Hovingh M, Noordzij W et al. Tumour necrosis as assessed with ^{18}F-FDG PET is a potential prognostic marker in diffuse large B cell lymphoma independent of MYC rearrangements. *Eur Radiol* 2019; 29(11): 6018-28.
13. Zhang J, Qi Z, Ou W et al. Advances in the treatment of malignant ascites in China. *Support Care Cancer* 2024; 32(2): 97.
14. Ayantunde AA, Parsons SL. Pattern and prognostic factors in patients with malignant ascites: a retrospective study. *Ann Oncol* 2007; 18(5): 945-9.
15. Rakheja R, Makis W, Tulbah R et al. Necrosis on ^{18}F-FDG PET/CT correlates with prognosis and mortality in sarcomas. *Am J Roentgenol* 2013; 201(1): 170-7.
16. Nioche C, Orlhac F, Boughdad S et al. LIFEx: a freeware for Radiomic feature calculation in Multimodality Imaging to accelerate advances in the characterization of Tumor Heterogeneity. *Cancer Res* 2018; 78(16): 4786-9.
17. Yee PP, Li W. Tumor necrosis: A synergistic consequence of metabolic stress and inflammation. *Bioessays* 2021; 43(7): e2100029.
18. Baik SH, Seo JW, Kim JH et al. Prognostic Value of Cervical Nodal Necrosis Observed in Preoperative CT and MRI of Patients With Tongue Squamous Cell Carcinoma and Cervical Node Metastases. *Am J Roentgenol* 2019; 213(2): 437-43.
19. Li J, Zhao Q, Zhang Y et al. Prognostic value of quantitative cervical nodal necrosis burden on MRI in nasopharyngeal carcinoma and its role as a stratification marker for induction chemotherapy. *Eur Radiol* 2022; 32(11): 7710-21.
20. Eren G, Kupik O. Necrosis on staging ^{18}F-FDG PET/CT is associated with worse progression-free survival in patients with stage IIIB non-small cell lung cancer. *J Cancer Res Ther* 2022; 18(4): 971-6.
21. Pierallini A, Bonamini M, Pantano P et al. Radiological assessment of necrosis in glioblastoma: variability and prognostic value. *Neuroradiology* 1998; 40(3): 150-3.
22. Adams HJA, de Klerk JMH, Fijnheer R et al. Prognostic value of tumor necrosis at CT in diffuse large B-cell lymphoma. *Eur J Radiol* 2015; 84(3): 372-7.
23. Valk PE, Budinger TF, Levin VA et al. PET of malignant cerebral tumors after interstitial brachytherapy. *J Neurosurg* 1988; 69(6): 830-8.
24. Jiang C, Teng Y, Zheng Z et al. Value of total lesion glycolysis and cell-of-origin subtypes for prognostic stratification of diffuse large B-cell lymphoma patients. *Quant Imaging Med Surg* 2021; 11(6): 2509-20.
25. Islam P, Goldstein J, Flowers CR. PET-derived tumor metrics predict DLBCL response and progression-free survival. *Leuk Lymphoma* 2019; 60(8): 1965-71.
26. Sehn LH, Berry B, Chhanabhai M et al. The revised International Prognostic Index (R-IPI) is a better predictor of outcome than the standard IPI for patients with diffuse large B-cell lymphoma treated with R-CHOP. *Blood* 2007; 109(5): 1857-61.
27. Zhou Z, Sehn LH, Rademaker AW et al. An enhanced International Prognostic Index (NCCN-IPI) for patients with diffuse large B-cell lymphoma treated in the rituximab era. *Blood* 2014; 123(6): 837-42.

28. Rubello D, Colletti PM. SUV Harmonization Between Different Hybrid PET/CT Systems. *Clin Nucl Med* 2018; 43(11): 811-4.
29. Meignan M, Sasanelli M, Casasnovas RO et al. Metabolic tumour volumes measured at staging in lymphoma: methodological evaluation on phantom experiments and patients. *Eur J Nucl Med Mol Imaging* 2014; 41(6): 1113-22.